Strong coupling between two quantum dots and a photonic crystal cavity using magnetic field tuning

Hyochul Kim,[1] Deepak Sridharan,[1] Thomas C. Shen,[1] Glenn S. Solomon,[2] and Edo Waks[1,*]

[1]*Department of Electrical and Computer Engineering, IREAP, University of Maryland, College Park, Maryland 20742, USA and Joint Quantum Institute, University of Maryland, College Park, Maryland 20742, USA*

[2]*Joint Quantum Institute, National Institute of Standards and Technology, and University of Maryland, Gaithersburg, Maryland 20899, USA*

**edowaks@umd.edu*

Abstract: We demonstrate strong coupling between two indium arsenide (InAs) quantum dots (QDs) and a photonic crystal cavity by using a magnetic field as a frequency tuning method. The magnetic field causes a red shift of an exciton spin state in one QD and a blue shift in the opposite exciton spin state of the second QD, enabling them to be simultaneously tuned to the same cavity resonance. This method can match the emission frequency of two QDs separated by detunings as large as 1.35 meV using a magnetic field of up to 7 T. By controlling the detuning between the two QDs we measure the vacuum Rabi splitting (VRS) both when the QDs are individually coupled to the cavity, as well as when they are coupled to the cavity simultaneously. In the latter case the oscillator strength of two QDs shows a collective behavior, resulting in enhancement of the VRS as compared to the individual cases. Experimental results are compared to theoretical calculations based on the solution to the full master equation and found to be in excellent agreement.

OCIS codes: (230.3810) Magneto-optic systems; (230.5298) Photonic crystals; (270.5580) Quantum electrodynamics.

References and links

1. J. P. Reithmaier, G. Sęk, A. Löffler, C. Hofmann, S. Kuhn, S. Reitzenstein, L. V. Keldysh, V. D. Kulakovskii, T. L. Reinecke, and A. Forchel, "Strong coupling in a single quantum dot-semiconductor microcavity system," Nature **432**, 197–200 (2004).
2. T. Yoshie, A. Scherer, J. Hendrickson, G. Khitrova, H. M. Gibbs, G. Rupper, C. Ell, O. B. Shchekin, and D. G. Deppe, "Vacuum Rabi splitting with a single quantum dot in a photonic crystal nanocavity," Nature **432**, 200–203 (2004).
3. E. Peter, P. Senellart, D. Martrou, A. Lemaître, J. Hours, J. M. Gérard, and J. Bloch, "Exciton-photon strong-coupling regime for a single quantum dot embedded in a microcavity," Phys. Rev. Lett. **95**, 067401 (2005).
4. E. Waks and J. Vučković, "Dipole induced transparency in drop-filter cavity-waveguide systems," Phys. Rev. Lett. **96**, 153601 (2006).
5. D. Englund, A. Faraon, I. Fushman, N. Stoltz, P. Petroff, and J. Vučković, "Controlling cavity reflectivity with a single quantum dot," Nature **450**, 857–861 (2007).
6. I. Fushman, D. Englund, A. Faraon, N. Stoltz, P. Petroff, and J. Vučković, "Controlled phase shifts with a single quantum dot," Science **320**, 769 (2008).
7. D. Bouwmeester, A. Ekert and A. Zeilinger, *The Physics of Quantum Information* (Springer, 2000).

#140623 - $15.00 USD Received 5 Jan 2011; revised 15 Jan 2011; accepted 19 Jan 2011; published 26 Jan 2011

8. A. Imamoğlu, D. D. Awschalom, G. Burkard, D. P. DiVincenzo, D. Loss, M. Sherwin, and A. Small, "Quantum information processing using quantum dot spins and cavity QED," Phys. Rev. Lett. **83**, 4204–4207 (1999).
9. J. Metz, M. Trupke, and A. Beige, "Robust entanglement through macroscopic quantum jumps," Phys. Rev. Lett. **97**, 040503 (2006).
10. Y. F. Xiao, J. Gao, X. B. Zou, J. F. Mcmillan, X. Yang, Y. L. Chen, Z. F. Han, G. C. Guo, and C. W. Wong, "Coupled quantum electrodynamics in photonic crystal cavities towards controlled phase gate operations," N. J. Phys. **10**, 123013 (2008).
11. S.-B. Zheng and G.-C. Guo, "Efficient scheme for two-atom entanglement and quantum information processing in cavity QED," Phys. Rev. Lett. **85**, 2392–2395 (2000).
12. D. Sridharan and E. Waks, "Generating entanglement between quantum dots with different resonant frequencies based on dipole-induced transparency," Phys. Rev. A **78**, 052321 (2008).
13. J. I. Cirac, P. Zoller, H. J. Kimble, and H. Mabuchi, "Quantum state transfer and entanglement distribution among distant nodes in a quantum network," Phys. Rev. Lett. **78**, 3221 (1997).
14. A. Serafini, S. Mancini, and S. Bose, "Distributed quantum computation via optical fibers," Phys. Rev. Lett. **96**, 010503 (2006).
15. S. Reitzenstein, A. Löffler, C. Hofmann, A. Kubanek, M. Kamp, J. P. Reithmaier, A. Forchel, V. D. Kulakovskii, L. V. Keldysh, I. V. Ponomarev, and T. L. Reinecke, "Coherent photonic coupling of semiconductor quantum dots," Opt. Lett. **31**, 1738–1740 (2006).
16. A. Faraon, D. Englund, I. Fushman, J. Vučković, N. Stoltz, and P. Petroff, "Local quantum dot tuning on photonic crystal chips," Appl. Phys. Lett. **90**, 213110 (2007).
17. S. Seidl, M. Kroner, A. Hogele, K. Karrai, R. J. Warburton, A. Badolato, and P. M. Petroff, "Effect of uniaxial stress on excitons in a self-assembled quantum dot," Appl. Phys. Lett. **88**, 203113 (2006).
18. H. Kim, S. M. Thon, P. M. Petroff, and D. Bouwmeester, "Independent tuning of quantum dots in a photonic crystal cavity," Appl. Phys. Lett. **95**, 243107 (2009).
19. A. Laucht, J. M. Villas-Bôas, S. Stobbe, N. Hauke, F. Hofbauer, G. Böhm, P. Lodahl, M.-C. Amann, M. Kaniber, and J. J. Finley, "Mutual coupling of two semiconductor quantum dots via an optical nanocavity," Phys. Rev. B **82**, 075305 (2010).
20. H. Kim, D. Sridharan, T. C. Shen, G. S. Solomon, and E. Waks, http://arxiv.org/abs/1101.0749 (2011).
21. S. Reitzenstein, S. Münch, P. Franeck, A. Rahimi-Iman, A. Löffler, S. Höfling, L. Worschech, and A. Forchel, "Control of the strong light-matter interaction between an elongated $In_{0.3}Ga_{0.7}As$ quantum dot and a micropillar cavity using external magnetic fields," Phys. Rev. Lett. **103**, 127401 (2009).
22. S. Reitzenstein, S. Münch, P. Franeck, A. Löffler, S. Höfling, L. Worschech, A. Forchel, I. V. Ponomarev, and T. L. Reinecke, "Exciton spin state mediated photon-photon coupling in a strongly coupled quantum dot microcavity system," Phys. Rev. B **82**, 121306 (2010).
23. J. M. Fink, R. Bianchetti, M. Baur, M. Göppl, L. Steffen, S. Filipp, P. J. Leek, A. Blais, and A. Wallraff, "Dressed collective qubit states and the Tavis-Cummings model in circuit QED," Phys. Rev. Lett. **103**, 083601 (2009).
24. Y. Akahane, T. Asano, B.-S. Song, and S. Noda, "Fine-tuned high-Q photonic-crystal nanocavity," Opt. Express **13**, 1202 (2005).
25. M. Bayer, G. Ortner, O. Stern, A. Kuther, A. A. Gorbunov, A. Forchel, P. Hawrylak, S. Fafard, K. Hinzer, T. L. Reinecke, S. N. Walck, J. P. Reithmaier, F. Klopf, and F. Schäfer, "Fine structure of neutral and charged excitons in self-assembled In(Ga)As/(Al)GaAs quantum dots," Phys. Rev. B **65**, 195315 (2002).
26. P. Michler, *Single Semiconductor Quantum Dots*, (Springer-Verlag Berlin Heidelberg, 2009).
27. M. Tavis and F. W. Cummings, "Exact solution for an *N*-molecule—radiation-field Hamiltonian," Phys. Rev. **170**, 379 (1968).
28. M. Winger, T. Volz, G. Tarel, S. Portolan, A. Badolato, K. J. Hennessy, E. L. Hu, A. Beveratos, J. Finley, V. Savona, and A. Imamoğlu, "Explanation of photon correlations in the far-off-resonance optical emission from a quantum-dot–cavity system," Phys. Rev. Lett. **103**, 207403 (2009).
29. S. Strauf, K. Hennessy, M. T. Rakher, Y. S. Choi, A. Badolato, L. C. Andreani, E. L. Hu, P. M. Petroff, and D. Bouwmeester, "Self-tuned quantum dot gain in photonic crystal lasers," Phys. Rev. Lett. **96**, 127404 (2006).
30. U. Hohenester, A. Laucht, M. Kaniber, N. Hauke, A. Neumann, A. Mohtashami, M. Seliger, M. Bichler, and J. J. Finley, "Phonon-assisted transitions from quantum dot excitons to cavity photons," Phys. Rev. B **80**, 201311 (2009).
31. S. M. Tan, "A computational toolbox for quantum and atomic optics," J. Opt. B **1**, 424 (1999).
32. P. Borri, W. Langbein, S. Schneider, U. Woggon, R. L. Sellin, D. Ouyang, and D. Bimberg, "Ultralong dephasing time in InGaAs quantum dots," Phys. Rev. Lett. **87**, 157401 (2001).

1. Introduction

Quantum dots (QDs) coupled to optical microcavities provide an ideal material system for studying cavity quantum electrodynamics (cQED). Recent improvements in fabrication and design of optical microcavities have enabled the study of the strong coupling regime of cQED

#140623 - $15.00 USD Received 5 Jan 2011; revised 15 Jan 2011; accepted 19 Jan 2011; published 26 Jan 2011

where the QD and optical mode mix to form new quasi-particles called polaritons [1–3]. Such strong light-matter interactions enable nonlinear optics near the single photon level [4–6], and have potential applications in the areas of quantum networking and quantum information [7,8].

The majority of experiments to date have focused on the study of a single QD coupled to a microcavity. Moving beyond single QDs to multiple QD systems is an important next step for various quantum information applications [7–15]. The study of multiple QD systems has remained technically challenging due to their wide spectral variations, making it extremely unlikely that two QDs will be resonant with the same cavity mode simultaneously. To overcome this problem we require methods to individually tune multiple QDs to the same frequency. Conventional tuning methods based on temperature [2,16] or strain [17] are not adequate because they affect all QDs identically, and do not provide individual tunability of QD frequencies. Recently, it has been shown that the DC Stark shift can be used to tune two QDs to the same frequency either by applying a separate electric bias to each QD using multi-layer diode structures [18], or by exploiting different voltage-dependent DC stark shifts between two QDs [19]. The latter approach has already been used to tune two QDs to the same cavity mode in the strong coupling regime.

In this work, we present a different method which uses a magnetic field to tune two QD exciton spin states into resonance, and demonstrate strong coupling between two QDs and a photonic crystal cavity. In the presence of a magnetic field, the QD exciton spin states can be split by the Zeeman effect, creating a red shift for one spin state and a blue shift for the other [20–22]. By matching the red shifted emission from one QD with the blue shifted emission from another, this method provides a way to tune two QDs into resonance over a large tuning range (1.35 meV with a 7 T magnetic field for indium arsenide (InAs) QDs). A major advantage of this approach is that it does not require the incorporation of a diode structure, eliminating the need for including highly doped layers in the cavity structure. Such layers lead to additional cavity losses due to free carrier absorption, reducing the cavity quality factor (Q). By using a combination of magnetic field tuning and temperature tuning, we are able to investigate both the large detuning regime, where we can characterize the coupling of the QDs individually to the cavity, and the small detuning regime where the QDs couple collectively. The collective behavior is demonstrated experimentally by an increased vacuum Rabi splitting (VRS) in the collective coupling relative to the individual coupling, similar to the recent demonstration in a circuit QED system [23]. We also investigate the fine features of the collective coupling regime when the QDs are detuned by a small amount relative to the cavity linewidth. Experimental results are compared to numerical simulation based on the solution to the full master equation and found to be in excellent agreement.

2. Experiment

We investigate gallium arsenide (GaAs) photonic crystal cavity devices that are coupled to InAs QDs. The initial sample consists of a 160 nm thick GaAs membrane with a single layer of InAs QDs in the middle, grown on top of a 1 μm thick $Al_{0.78}Ga_{0.22}As$ sacrificial layer. InAs QDs with uniform density of $10-30/\mu m^2$ are grown by depositing 1.7 monolayer of InAs while rotating the wafer during growth. In addition, the in-situ annealing is used to blue shift the emission wavelength of the QDs to $900-950$ nm. Photonic crystal cavities are patterned into the membrane by electron beam lithography and dry etching, followed by a chemical wet etch to remove the sacrificial layer resulting in a suspended membrane structure. A scanning electron microscope (SEM) image of a sample photonic crystal structure is shown in the inset to Fig. 1a. The cavity design is based on a three hole defect (L3) cavity with three hole tuning in order to optimize the cavity Q [24].

The sample was mounted in a continuous flow liquid helium cryostat and a magnetic field of

#140623 - $15.00 USD Received 5 Jan 2011; revised 15 Jan 2011; accepted 19 Jan 2011; published 26 Jan 2011

up to 7 T was applied by a superconducting magnet. All data in this experiment was taken with the magnetic field parallel to the sample growth direction (Faraday configuration). Photoluminescence (PL) measurements were obtained by exciting the sample using a Ti:Sapphire laser tuned to 865 nm. Sample excitation and collection were performed with a confocal microscope using an objective lens with numerical aperture of 0.68. Spectral measurements were performed using a grating spectrometer with a resolution of 0.02 nm.

Figure 1a shows a PL spectrum obtained from a specific photonic crystal structure at a sample temperature of 28 K. The emission spectrum exhibits a bright peak due to the cavity emission, along with several weaker peaks corresponding to emission from different QDs. In particular, we focus on two specific QDs labeled X_1 and X_2 in the figure. The emission from these QDs exhibits hyperfine splitting due to the electron-hole exchange interaction in asymmetric QDs [25], resulting in two closely spaced peaks for each X_1 and X_2. The hyperfine splitting ensures that X_1 and X_2 correspond to neutral excitonic emission, as opposed to emission from charged excitons where both the exchange energies and hyperfine splitting vanish [25]. From the linear power dependence of the emission we verify that X_1 and X_2 correspond to single exciton states from two independent QDs rather than an exciton and biexciton manifold of a single QD, where the biexciton would exhibit quadratic power dependence [26]. By fitting the emission of the cavity to a Lorentzian, we determine the cavity linewidth to be 0.105 nm, which corresponds to a Q of 9,000.

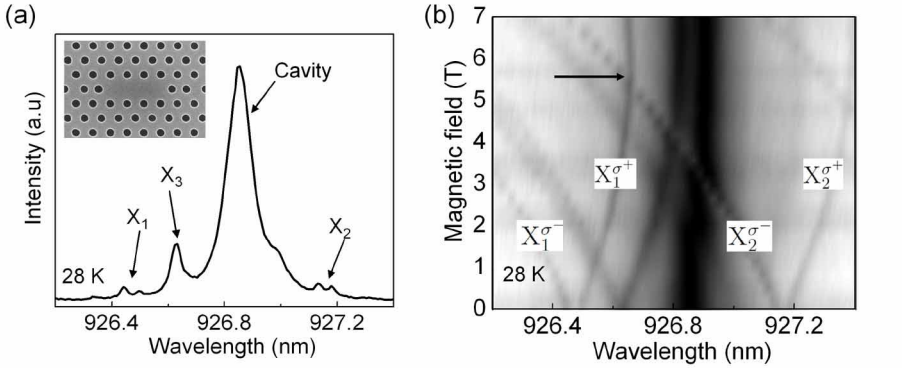

Fig. 1. (a) PL spectrum of a photonic crystal cavity and coupled QDs at 0 T. The QD with the emission wavelength at 926.47 ± 0.03 nm is designated as X_1, the one at 927.16 ± 0.02 nm as X_2, the one at 926.63 nm as X_3, and the cavity mode is at 926.85 nm. Both X_1 and X_2 show two split emission lines due to the electron-hole exchange interaction existing in neutral excitons of asymmetric QDs. (b) Cavity spectra as a function of applied magnetic field. Each QD emission line splits into two circularly polarized branches due to the Zeeman effect. The arrow indicates when two QD exciton spin states $X_1^{\sigma^+}$ and $X_2^{\sigma^-}$ are tuned into resonance with each other. At this point the two QDs are detuned from the cavity by 0.21 nm.

When we apply a magnetic field, each of the exciton lines splits into two branches with circularly polarized emission due to the Zeeman effect. We denote these two polarizations as $\sigma^{\pm}$, where σ^+ (σ^-) corresponds to the emission from the exciton with an electron of spin $-1/2$ ($1/2$) and a hole of spin $3/2$ ($-3/2$). Figure 1b shows the measured PL spectra from the same device shown in Fig. 1a as a function of the magnetic field strength. The spectra are measured from 0 T to 7 T with 0.3 T steps. At 0 T, the emission energy of QDs X_1 and X_2

#140623 - $15.00 USD Received 5 Jan 2011; revised 15 Jan 2011; accepted 19 Jan 2011; published 26 Jan 2011

are separated by 0.69 nm. As the magnetic field is increased, the lower energy branch of X_1, denoted $X_1^{\sigma^+}$, and the higher energy branch of X_2, denoted $X_2^{\sigma^-}$, approach each other and can be tuned into resonance. At a fixed temperature of 28 K and a magnetic field of 5.5 T, $X_1^{\sigma^+}$ and $X_2^{\sigma^-}$ are resonant with each other (as indicated by the arrow), but detuned from the cavity by 0.21 nm. These measurements show that by changing the magnetic field, we can control the relative energy separation between $X_1^{\sigma^+}$ and $X_2^{\sigma^-}$ over a relatively large range.

We first examine the regime where the two exciton spin states are highly detuned from each other so that we can characterize how they couple to the cavity individually. We set the magnetic field to 2.4 T where $X_1^{\sigma^+}$ and $X_2^{\sigma^-}$ are separated from each other in emission wavelength by 0.36 nm, which is larger than the cavity linewidth. At a temperature below 25 K, $X_1^{\sigma^+}$ and $X_2^{\sigma^-}$ are both blue detuned from the cavity mode. By increasing the temperature each of the QD emission lines red shifts faster than the cavity mode frequency and eventually overtakes it. Figure 2a plots the emission spectra as a function of temperature. The $X_1^{\sigma^+}$ emission is tuned to cavity resonance at a temperature of 37 K, while the $X_2^{\sigma^-}$ is resonant with the cavity at 27 K. As each excitation becomes resonant with the cavity mode, a clear anti-crossing behavior is observed indicating that both QDs are coupled to the cavity in the strong coupling regime. In addition to these two resonances, several other QD lines (such as the emission from X_3) are observed to strongly couple with the cavity mode.

Figure 2b shows a series of cavity spectra in the temperature range of $34-40$ K, where the emission from $X_1^{\sigma^+}$ is close to cavity resonance. As the $X_1^{\sigma^+}$ is tuned through the cavity mode, a clear anti-crossing behavior is observed. The minimum energy separation between the two polariton modes is $\Delta E = 86\ \mu$eV, attained at a temperature of 37 K. We attain this value fitting the spectrum to a sum of two Lorentzian functions and determining the separation of these two fitted peaks. Fig. 2c shows a similar series of spectra at the temperature range of $24-30$ K, where $X_2^{\sigma^-}$ is now nearly resonant with the cavity mode. The minimum energy separation is obtained at 27 K, and is given by $\Delta E = 96\ \mu$eV. From the minimum energy splitting we can

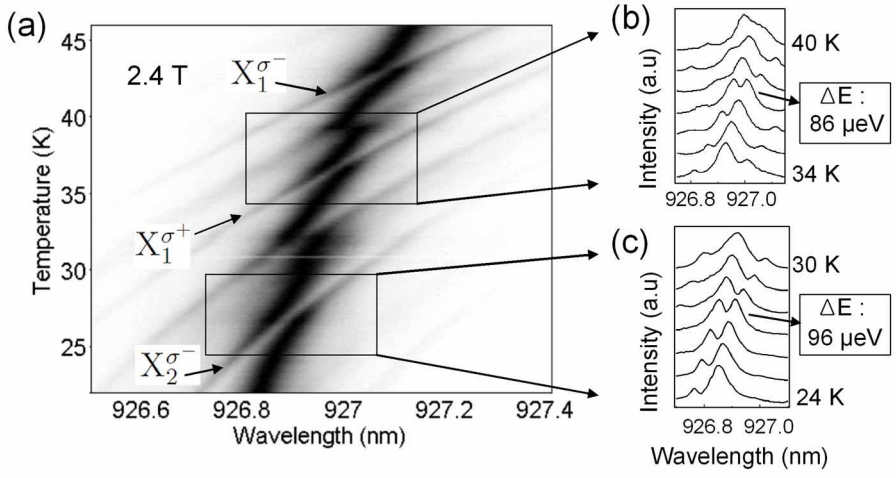

Fig. 2. (a) Cavity emission spectra as a function of temperature at a magnetic field of 2.4 T. (b) Series of spectra taken at a temperature range of $34-40$ K where $X_1^{\sigma^+}$ is close to cavity resonance. (c) Series of spectra taken from $24-30$ K where $X_2^{\sigma^-}$ is nearly resonant with the cavity. For both panels b and c, ΔE denotes the minimum energy separation between the two polaritons, achieved when the cavity and QD emission are resonant.

#140623 - $15.00 USD Received 5 Jan 2011; revised 15 Jan 2011; accepted 19 Jan 2011; published 26 Jan 2011

directly calculate the exciton-photon coupling strength g using the equation

$$g = \sqrt{\frac{\Delta E^2}{4\hbar^2} + \frac{(\gamma_c - \gamma_x)^2}{16}} \tag{1}$$

where γ_c and γ_x are the cavity and exciton decay rates respectively. From the cavity Q we can determine the cavity mode decay rate to be $\gamma_c = \omega_c/2\pi Q = 36.4$ GHz while the exciton linewidth is given by $\gamma_x = 0.16$ GHz which is negligibly small compared to the cavity linewidth. From Eq. (1), we obtain $g_1 = 13.8$ GHz and $g_2 = 14.8$ GHz where g_1 and g_2 are the exciton-photon coupling strengths of states $X_1^{\sigma^+}$ and $X_2^{\sigma^-}$, respectively.

Next, we investigate the collective coupling behavior of two QDs when they are tuned into resonance with the cavity. The magnetic field is adjusted to the level where $X_1^{\sigma^+}$ and $X_2^{\sigma^-}$ are nearly on resonance with each other. We perform a temperature scan at magnetic fields of 5.9 T, 5.75 T and 5.5 T, as shown in Fig. 3a-c. The wavelength separations between the two QDs are 0.055 nm at 5.9 T, 0.035 nm at 5.75 T, and negligible (below the resolution of the spectrometer) at 5.5 T. When the wavelength separations of the two QD emission lines are non-negligible (panels a and b), three clear peaks are observed as the two QD excitons are scanned across the cavity mode. As the magnetic field is tuned from 5.9 T to 5.75 T the detuning is decreased and simultaneously the middle peak becomes weaker. As the magnetic field is further reduced to 5.5 T and the QD detuning becomes negligible, the middle peak is fully suppressed and we recover a spectral doublet similar to the case where each QD was individually coupled to the cavity.

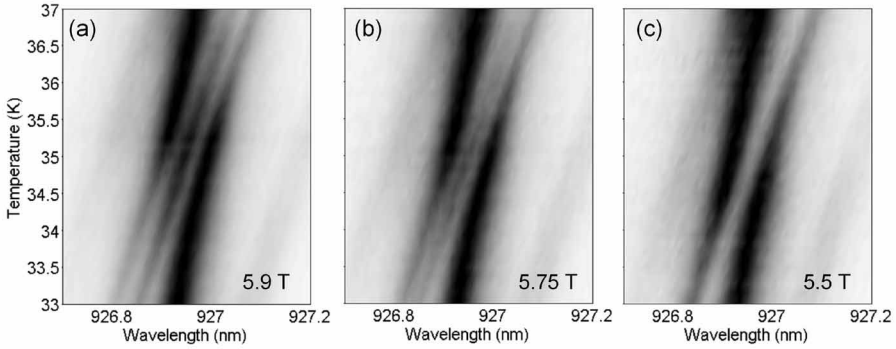

Fig. 3. Measured PL spectra when two QDs are simultaneously coupled to a cavity as a function of temperature at three different magnetic field strengths. The magnetic field strengths (and corresponding separations between the two QD emission wavelengths) are (a) 5.9 T (0.055 nm), (b) 5.75 T (0.035 nm), and (c) 5.5 T (0 nm).

To investigate the near-resonant condition more carefully, we perform spectral measurements where the emission frequency of the $X_1^{\sigma^+}$ exciton emission is nearly fixed at the cavity resonant frequency of $\lambda_c = 926.94$ nm while the $X_2^{\sigma^-}$ exciton is tuned through the cavity resonance. To achieve this condition we measure spectra of the device at 34 K while sweeping the magnetic field from 5 T to 5.9 T. Above 5 T, the emission frequency of the σ^+ exciton line stays nearly constant because the Zeeman and diamagnetic shifts are in opposite directions and cancel out, while the σ^- exciton line exhibits a very strong dependence because the two shifts are both in the same direction. By fitting spectral change of uncoupled QDs as a function of magnetic field, we observe that between $5 - 5.9$ T, the change of the emission wavelength of the $X_1^{\sigma^+}$ exciton is less than 0.01 nm while the $X_2^{\sigma^-}$ exciton emission shifts about 0.106 nm, as can be seen in

#140623 - $15.00 USD Received 5 Jan 2011; revised 15 Jan 2011; accepted 19 Jan 2011; published 26 Jan 2011

Fig. 1b. At a temperature of 34 K, the emission frequency of the $X_1^{\sigma^+}$ exciton is resonant with the cavity at magnetic fields of $5-5.9$ T. We then tune the $X_2^{\sigma^-}$ emission through the cavity mode by increasing the magnetic field while minimally shifting the emission of the $X_1^{\sigma^+}$.

Figure 4a shows the spectra as a function of magnetic field at a fixed temperature of 34 K. The magnetic field is swept from $5-5.9$ T in steps of 0.05 T. At 5.9 T, we observe three clear emission lines; the emission line of $X_2^{\sigma^-}$ and two peaks due to the anti-crossing between $X_1^{\sigma^+}$ and a cavity. By decreasing the magnetic field from 5.9 T to 5.5 T, $X_2^{\sigma^-}$ approaches the cavity mode and the middle peak is suppressed similar to the spectra shown in Fig. 3c. The measured minimum energy separation at 5.5 T is 119 μeV, which corresponds to a collective cavity-QD coupling strength of 17.1 GHz. The energy separation when both QDs are resonantly coupled to the cavity is larger than the energy separation of the individual QDs. This increased splitting is the signature of collective interaction between the two QDs and the cavity.

3. Theory and discussion

In order to explain the experimental results, we model the QDs as two independent two-level systems interacting with a single cavity mode. The emission frequencies of the QDs are designated by ω_1 and ω_2 and the cavity resonant frequency is denoted as ω_c. The coupling strengths of each QD with a cavity are given by g_1 and g_2, respectively. When two dipole emitters are coupled to a single cavity mode, the system Hamiltonian is described by the Tavis-Cummings model [27]:

$$\mathbf{H} = \hbar\omega_c \mathbf{a}^\dagger \mathbf{a} + \frac{\hbar}{2}(\omega_1 \sigma_{\mathbf{1z}} + \omega_2 \sigma_{\mathbf{2z}}) + \hbar g_1(\sigma_{\mathbf{1}+}\mathbf{a} + \mathbf{a}^\dagger \sigma_{\mathbf{1}-}) + \hbar g_2(\sigma_{\mathbf{2}+}\mathbf{a} + \mathbf{a}^\dagger \sigma_{\mathbf{2}-}), \qquad (2)$$

where $\sigma_{\mathbf{1}-}$ and $\sigma_{\mathbf{2}-}$ ($\sigma_{\mathbf{1}+}$ and $\sigma_{\mathbf{2}+}$) represent the dipole lowering (raising) operators for QD1 and QD2, $\sigma_{\mathbf{1z}}$ and $\sigma_{\mathbf{2z}}$ are Pauli operators corresponding to the population difference between

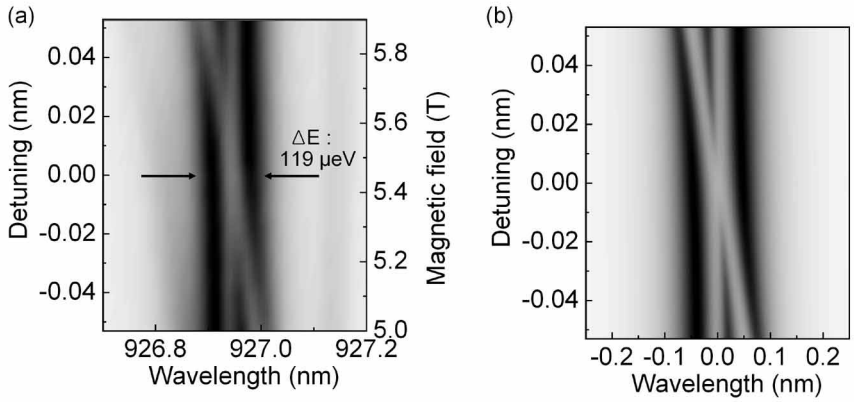

Fig. 4. (a) Experimental measurement of VRS with two QDs strongly coupled to a cavity. $X_1^{\sigma^+}$ is kept nearly constant and strongly coupled to the cavity, and the $X_2^{\sigma^-}$ emission frequency is swept through the cavity mode by decreasing the magnetic field from 5.9 T to 5 T . The minimum energy separation between two resonant QDs and the cavity is 119 μeV. (b) Numerical simulation of VRS with two QDs strongly coupled to a cavity. One strongly coupled QD is kept at resonance with a cavity, and another strongly coupled QD emission wavelength is tuned through the cavity mode.

#140623 - $15.00 USD Received 5 Jan 2011; revised 15 Jan 2011; accepted 19 Jan 2011; published 26 Jan 2011

the excited and ground state, and the operator $\mathbf{a}$ ($\mathbf{a}^\dagger$) is the photon annihilation (creation) operator for the cavity.

In the weak excitation limit we can consider only the lowest three excited states of the Hamiltonian, denoted $|e,g,0\rangle$, $|g,e,0\rangle$ and $|g,g,1\rangle$. The first two states correspond to the case where there is no photon in the cavity and one of the QDs is in the excited state, denoted e, while the other is in the ground state, denoted g. The state $|g,g,1\rangle$ corresponds to the case where both QDs are in the ground state and one photon exists in the cavity. With these three states, Eq. (2) can be represented in 3×3 matrix form as

$$\mathbf{H} = \hbar \begin{bmatrix} \frac{1}{2}(\omega_1-\omega_2) & 0 & g_1 \\ 0 & -\frac{1}{2}(\omega_1-\omega_2) & g_2 \\ g_1 & g_2 & \omega_c - \frac{1}{2}\omega_1 - \frac{1}{2}\omega_2 \end{bmatrix} \tag{3}$$

The Hamiltonian matrix has non-diagonal terms due to the QD-cavity coupling terms g_1 and g_2. We can calculate the energy eigenstates and eigenvalues of this system by diagonalizing this Hamiltonian matrix.

To get an intuitive understanding for the behavior of the system, we first consider the special case where the coupling strength of the two QDs is the same ($g_0 = g_1 = g_2$) and both QDs are resonant with the cavity mode ($\omega_1 = \omega_2 = \omega_c$). The obtained energy eigenstates of Eq. (3) are $(|e,g,0\rangle + |g,e,0\rangle - \sqrt{2}|g,g,1\rangle)/2$, $(|e,g,0\rangle - |g,e,0\rangle)/\sqrt{2}$ and $(|e,g,0\rangle + |g,e,0\rangle + \sqrt{2}|g,g,1\rangle)/2$, with corresponding energy eigenvalues $-\sqrt{2\hbar}g_0$, 0 and $\sqrt{2\hbar}g_0$. One of the eigenstates, $|\psi_d>= (|e,g,0\rangle - |g,e,0\rangle)/\sqrt{2}$, is a dark state because it does not couple to the state $|g,g,0\rangle$ (the system ground state) by dipole radiation and cavity decay [23]. The two remaining states are bright states that can decay to the system ground state both by dipole radiation and cavity decay. Their energy difference is given by $\Delta = 2\sqrt{2\hbar}g_0$, which is a factor of $\sqrt{2}$ larger than the energy separation when each QD is individually coupled to the cavity mode.

For the more general case where $g_1 \neq g_2$, we still obtain two bright states and a dark state, but now the dark state can partially radiate due to imperfect destructive interference between the two dipole emitters. The new energies are given by $-\hbar\sqrt{g_1^2+g_2^2}$, 0, and $\hbar\sqrt{g_1^2+g_2^2}$, and the effective splitting between the two bright transitions is $\Delta = 2\hbar g_c = 2\hbar\sqrt{g_1^2+g_2^2}$, where g_c is defined as the collective coupling strength. The experimentally measured individual coupling strengths of $X_1^{\sigma^+}$ and $X_2^{\sigma^-}$ are given by $g_1 = 13.8$ GHz and $g_2 = 14.8$ GHz, as previously measured in Fig. 2. From these numbers the theoretically predicted collective coupling strength is given by $g_c = 20.2$ GHz, while the measured collective coupling strength, determined from Fig. 4a, is $g_c = 17.1$ GHz. We observe a reduction of 16% in the measured collective coupling strength as compared to the collective coupling strength calculated from the individual coupling strengths. This disagreement may be attributed to the fact that the individual coupling strength and collective coupling strength are measured at different magnetic fields and temperatures. In previous work we have shown that the coupling strength of a single QD state and a cavity exhibited a small change with magnetic field [20]. Since the individual QD coupling strengths were measured at 2.4 T and the collective coupling strength was measured at 5.5 T, this magnetic field dependence may explain the discrepancy.

In the theoretical discussion above, we have considered the ideal case in which there is no loss in the system. In order to create a more realistic model that properly accounts for cavity and dipole damping, we consider the solution to the full master equation given by $\frac{d\rho}{dt} = -\frac{i}{\hbar}[\mathbf{H},\rho] + \mathbf{L}\rho$, where ρ is the density matrix of the system, $\mathbf{H}$ is the Hamiltonian defined in Eq. (2), and $\mathbf{L}$ is the Liouvillian superoperator. The Hamiltonian describes the processes leading to the reversible exchange of energy between the cavity and the QDs. The Liouvillian operator $\mathbf{L}$ represents the irreversible decays and incoherent pumping to the system, and can be written as

#140623 - $15.00 USD Received 5 Jan 2011; revised 15 Jan 2011; accepted 19 Jan 2011; published 26 Jan 2011

$\mathbf{L} = \mathbf{L_{cav}} + \mathbf{L_{QD}} + \mathbf{L_{dephase}} + \mathbf{L_{pump-QD}} + \mathbf{L_{pump-cav}}$, where $\mathbf{L_{cav}}$ represents cavity decay, $\mathbf{L_{QD}}$ accounts for dipole decay of the QD excitons, $\mathbf{L_{dephase}}$ accounts for dephasing of QD excitons, $\mathbf{L_{pump-QD}}$ represents incoherent pumping of the QDs and $\mathbf{L_{pump-cav}}$ accounts for incoherent pumping of the cavity from other non-resonant QDs [19,28–30]. These operators are defined as follows:

$$\mathbf{L_{cav}}\rho = \frac{\gamma_c}{2}\left(2\mathbf{a}\rho\mathbf{a}^\dagger - \mathbf{a}^\dagger\mathbf{a}\rho - \rho\mathbf{a}^\dagger\mathbf{a}\right), \tag{4}$$

$$\mathbf{L_{QD}}\rho = \sum_{i=1,2}\left[\frac{\gamma_i}{2}\left(2\sigma_{\mathbf{i}-}\rho\sigma_{\mathbf{i}+} - \sigma_{\mathbf{i}+}\sigma_{\mathbf{i}-}\rho - \rho\sigma_{\mathbf{i}+}\sigma_{\mathbf{i}-}\right)\right], \tag{5}$$

$$\mathbf{L_{dephase}}\rho = \sum_{i=1,2}\left[\frac{\beta_i}{2}\left(2\sigma_{\mathbf{i}+}\sigma_{\mathbf{i}-}\rho\sigma_{\mathbf{i}+}\sigma_{\mathbf{i}-} - \sigma_{\mathbf{i}+}\sigma_{\mathbf{i}-}\rho - \rho\sigma_{\mathbf{i}+}\sigma_{\mathbf{i}-}\right)\right], \tag{6}$$

$$\mathbf{L_{pump-QD}}\rho = \sum_{i=1,2}\left[\frac{P_{QD}}{2}\left(2\sigma_{\mathbf{i}+}\rho\sigma_{\mathbf{i}-} - \sigma_{\mathbf{i}-}\sigma_{\mathbf{i}+}\rho - \rho\sigma_{\mathbf{i}-}\sigma_{\mathbf{i}+}\right)\right], \tag{7}$$

$$\mathbf{L_{pump-cav}}\rho = \frac{P_c}{2}\left(2\mathbf{a}^\dagger\rho\mathbf{a} - \mathbf{a}\mathbf{a}^\dagger\rho - \rho\mathbf{a}\mathbf{a}^\dagger\right) \tag{8}$$

In Eqs. (4)–(8), γ_c is the cavity loss rate, γ_i is a radiative loss rate of the i'th QD, β_i represents a dephasing rate of the i'th QD, P_{QD} is the incoherent pumping rate of the QDs and P_c is the incoherent pumping rate of the cavity.

Calculations are performed using quantum regression theorem to calculate the power spectrum of the cavity field. The two-time covariance function $\langle \mathbf{a}^\dagger(t+\tau), \mathbf{a}(t)\rangle$ is calculated in the steady state stationary limit (where $t \to \infty$), and then the power spectrum is obtained by taking the fourier transform. All calculations were performed using an open source quantum optics toolbox [31].

Numerical simulations were performed using the experimentally measured parameters for g_1, g_2 and cavity loss rate γ_c. To model the experiment described in Fig. 4a we keep one QD resonant with a cavity ($\omega_1 = \omega_c$), and sweep the second QD emission (ω_2) by 0.106 nm around ω_c. Figure 4b shows the simulation result with the parameters $g_1 = 11.6$ GHz, $g_2 = 12.4$ GHz, $\gamma_c = 36.4$ GHz, $\gamma_1 = \gamma_2 = 0.16$ GHz, $P_{QD} = 0.1$ GHz and $P_c = 2.4$ GHz . The coupling constants g_1 and g_2 were reduced by 16% to account for the reduction in collective coupling strength measured at 5.5 T. The QD dephasing rate was set to $\beta_i = 3.4$ GHz [32], P_{QD} was chosen to be low enough to ensure that the coupled QDs are not saturated, and P_c was chosen to account for the measured cavity signal which is dominant in the PL spectrum even when the cavity is not resonant with two strongly coupled QDs. The spectrum is plotted along the x-axis in terms of relative wavelength detuning from the cavity center wavelength, while the y-axis represents the wavelength detuning between two QDs. When the wavelength detuning of the two QDs is larger than 0.01 nm, all three peaks are clearly visible in the spectrum. However, when the two QDs are resonant, the middle peak is not visible and we observe only two emission lines, consistent with the experimental measurement. We note that the suppression of the middle peak in the experimental data occurs over a larger detuning range than the simulated data. This discrepancy is partially due to the spectrometer resolution limit, which is only 0.02 nm, and therefore cannot resolve the very sharp spectral features that occur at extremely small detunings. Another possible contribution is that the bare QD linewidth could be underestimated in the simulation. The QD linewidth was obtained from published temperature dependent dephasing rates [32]. These linewidths may not account for other broadening mechanisms such as temperature instability which will lead to slow spectral wandering.

#140623 - $15.00 USD Received 5 Jan 2011; revised 15 Jan 2011; accepted 19 Jan 2011; published 26 Jan 2011

4. Conclusion

In summary, we have demonstrated strong coupling between two QDs and a cavity using a magnetic field to tune the frequencies of two QDs into resonance. We exploit the large magnetic field tunability to investigate the individual coupling strength between single QDs and a photonic crystal cavity, as well as the collective coupling strength of the two QDs that are resonantly coupled to the cavity simultaneously. Experimental measurements for collective coupling strength of the two QDs and spectral dependence agree well with numerical simulation of the full master equation. The ability to tune two QDs onto the same cavity may find use for entanglement schemes in which a cavity mode is used to create quantum interactions between multiple atomic systems [11]. It can also be naturally extended to the situation where two QDs are tuned onto resonance with two different cavities, providing a route towards coupling and entanglement of spatially separated QDs using optical channels [12]. These types of devices would represent a first step towards solid-state based quantum networks [13] and quantum computers [14] using optically mediated entanglement operations.

Acknowledgements

The authors would like to acknowledge support from the ARO MURI on Hybrid quantum interactions (grant number W911NF09104), the Physics Frontier Center at the Joint Quantum Institute, and the ONR Applied Electromagnetics center. E. Waks would like to acknowledge support from an NSF CAREER award (grant number ECCS. 0846494).

#140623 - $15.00 USD Received 5 Jan 2011; revised 15 Jan 2011; accepted 19 Jan 2011; published 26 Jan 2011